

# Spindle Imbalance Detection Method Based on Principal Component Analysis and Self-Organizing Map for Computer Numerical Control Machine Tools

Hao Yu Lin\*, Ping Chun Tsai\*, Ping Cheng Lin\* and Jui Peng Hsu\*\*

**Keywords:** spindle monitoring, spindle imbalance, principal component analysis, self-organizing map

## ABSTRACT

This paper introduces a spindle imbalance detection method based on principal component analysis and a self-organizing map for machine tools under computer numerical control. By analyzing vibration signals collected during spindle operation, the method extracted eight key frequency-domain features, including spindle rotation and bearing characteristic frequencies. These features were refined through principal component analysis to eliminate collinearity while preserving essential information. A diagnostic model was established using a self-organizing map trained exclusively with healthy state data, enabling the autonomous monitoring of spindle health conditions. The method's effectiveness was validated through extensive experiments on a YCM\_NDV102A vertical machining center. Experiments revealed accuracy of 99.7% and 100% in identifying normal spindle conditions and imbalance states, respectively. Overall, the proposed method performed similarly to a supervised learning method but did not require fault data for model training, making it more suitable for industrial applications.

## INTRODUCTION

In modern manufacturing, spindle systems play a key role in the use of computer numerical control (CNC) machine tools because these systems' operation directly affects machining precision and

*Paper Received January, 2025. Revised April, 2025. Accepted April, 2025. Author for Correspondence: Ping Chun Tsai.*

\* Department of Mechanical Design Engineering, National Formosa University, Yunlin County, Taiwan (R.O.C.).

\* Department of Mechanical Design Engineering, National Formosa University, Yunlin County, Taiwan (R.O.C.).

\*\* Precision Machinery Research Development Center, Taichung, Taiwan (R.O.C.)

product quality. Detection of spindle imbalance is a major challenge in maintaining machining accuracy and extending equipment's lifespan. The traditional detection methods are primarily manual inspection and scheduled maintenance, which are time-consuming and require substantial human resources (Dai et al., 2022). These conventional approaches typically lack real-time monitoring capabilities, potentially leading to delayed fault detection and high maintenance costs (Cao et al., 2017; Wong et al., 2020). These limitations are particularly prominent in high-speed-machining environments, in which spindle imbalance can result in poor surface quality, accelerated tool wear, and even equipment safety concerns (Dai et al., 2022; Huang et al., 2015).

Recent advancements in condition monitoring technology have underscored the effectiveness of vibration signal analysis in detecting spindle imbalance. Vibration-based monitoring offers several advantages, including noninvasive measurement, real-time detection capability, and high sensitivity to mechanical anomalies (Gangsar and Tiwari, 2020). According to the literature, the vibration signals generated during a spindle's operation contain key information regarding the spindle's dynamic behavior, and these signals can be used to identify imbalance conditions before any severe damage occurs (Kuntoğlu et al., 2021). In addition, analyzing the spectral features of vibration signals can help identify various spindle fault modes, with imbalance fault characteristics being particularly distinctive modes (Hsieh et al., 2015). Moreover, integrating edge computing architecture can substantially improve the efficiency of data processing, enabling real-time fault detection (Wójcicki et al., 2021). Empirical mode decomposition can be used to process nonstationary vibration signals, and it can be combined with adaptive threshold recommendation to enhance detection accuracy (Olalere et al., 2023; Zheng et al., 2022). Deep learning technology can be employed for signal processing and feature extraction (Tama et al., 2023). Various vibration signal-based deep learning fault detection methods have been developed, including graph-based neural networks, physics-informed

machine learning, and transformer convolutional network-based fault diagnosis. However, these methods require large amounts of fault data for training, and obtaining these data is often difficult in industrial environments.

Intelligent diagnostic technology plays a key role in spindle health monitoring (Cao et al., 2017). Despite the potential of machine learning in spindle fault detection, most of the currently available machine learning methods rely on supervised learning (Fernandes et al., 2022). These methods typically require data from both healthy and faulty states for model training, which poses major limitations in practical applications in which fault data may be scarce or unavailable, thereby necessitating the development of more practical semisupervised or unsupervised learning techniques (Denkena et al., 2021). Many detection systems require manual parameter adjustment and threshold setting, which reduces their adaptability to wide-ranging operating conditions (Kuntoğlu et al., 2021; Olalere et al., 2023; Wójcicki et al., 2021; Zheng et al., 2022). Both automatic system parameter adjustment and adaptive threshold setting are crucial to improving a detection system's robustness (Thoppil et al., 2022). Methods combining multisource data and multiscale analysis can enhance detection reliability (Ma et al., 2023), although effectively integrating such information remains challenging. Additionally, maintaining high detection accuracy while reducing computational load in complex industrial environments remains an essential research task (Hassan et al., 2023). According to the latest research trends, digital twin technology can be applied to spindle health monitoring (Peng et al., 2022). Moreover, establishing accurate digital models integrated with real-time monitoring data can help predict spindle dynamic behavior and potential failures.

To address the aforementioned challenges, this paper introduces a spindle imbalance detection method (SIDM) that integrates principal component analysis (PCA) with a self-organizing map (SOM). This method involves extracting frequency-domain features from vibration signals, refining these features through PCA, and establishing a diagnostic model by using an SOM. Unlike traditional supervised learning techniques, this method requires only healthy state data to establish an effective detection mechanism. The effectiveness of the proposed method was demonstrated through experiments on a vertical machining center, and the results indicate its excellent detection performance.

The remainder of this paper is organized as follows. Section 2 describes the experimental setup and data collection process, including vibration signal measurements conducted using accelerometers installed on a vertical machining center spindle. Section 3 introduces the theoretical framework of the proposed method, including feature extraction, PCA-

based feature refinement, and SOM-based detection model development. Section 4 discusses the effectiveness of the proposed method, as shown through comprehensive experimental validation and a comparison with traditional supervised learning methods. Finally, Section 5 summarizes the main findings and contributions of this study.

## EXPERIMENTAL ANALYSIS

To validate the effectiveness of the proposed method, experiments were conducted using a YCM\_NDV102A vertical machining center. Because of the major effects of spindle vibration characteristics on machining precision and equipment lifespan, the experimental design prioritized the acquisition and analysis of accurate vibration signals. Data were collected at a sampling frequency of 12,800 Hz by using a single-axis accelerometer (model: PCB 601A02) installed on a spindle as shown in Figure 1. The specifications of the accelerometer and data acquisition module (model: NI 9234) are presented in Table 1 and Table 2, respectively. The spindle was operated at 10,000 RPM under no-load conditions, with each measurement of duration 1 s constituting a complete data record. Over a period of 1 month (from April 8 to May 9, 2024), 51,750 normal spindle operation data points and 1,800 unbalanced spindle operation data points were collected.

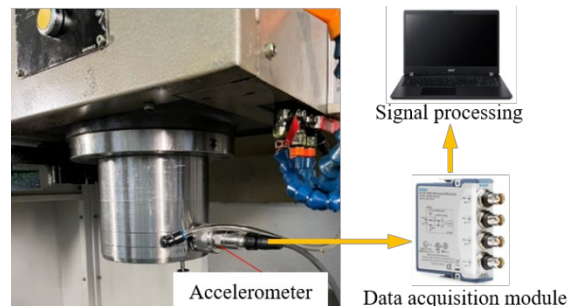


Fig. 1. Setup for accelerometer installation and data acquisition system configuration.

To train and validate our model, we simulated changes in spindle dynamic balance by replacing the locking screws on the terminal key, in accordance with the manufacturer's recommendations. The terminal key plays a crucial role in the entire spindle system, primarily ensuring accurate and secure installation of the tool holder in the spindle shaft (Figure 2(a)). When the tool holder is inserted into the spindle shaft, the keyway on the tool holder must precisely align with the terminal key fixed on the spindle shaft. A precise fit ensures effective and stable transmission of torque from the spindle to the tool holder during operation.

Table 1. Accelerometer specifications

Parameter	Value
Sensitivity	500 mV/g
Frequency range ( $\pm 3$ dB)	0.17 ~ 8000 Hz
Measuring range	$\pm 10$ g
Broadband Resolution	35 $\mu$ g

Table 2. Data acquisition module specifications

Parameter	Value
Input Range	$\pm 5$ V
Maximal Sampling rate	51.2 kHz
Resolution	24 bits
Built-in filter	Anti-aliasing filter

The experimental design defined the spindle state with standard-mass screws (5.3 g) installed as the healthy baseline state, representing the optimal

dynamic balance conditions during spindle operation. The standard screws were replaced with lighter screws (4.6 g) selected from the manufacturer's approved replacement parts list, and the mass difference of 0.7 g (representing a 13.2% reduction from the standard mass) resulted in a prominent dynamic imbalance in the spindle system (Figure 2(b)). This carefully controlled mass differential was sufficient to induce detectable dynamic imbalance while remaining within the manufacturer's safety parameters for experimental testing. Such an approach enabled the establishment of a complete data set containing different spindle operating states, providing a reliable experimental foundation for subsequent analyses and validation. This experimental design not only simulated potential spindle imbalance scenarios in actual working environments but also ensured experimental controllability and data reproducibility.

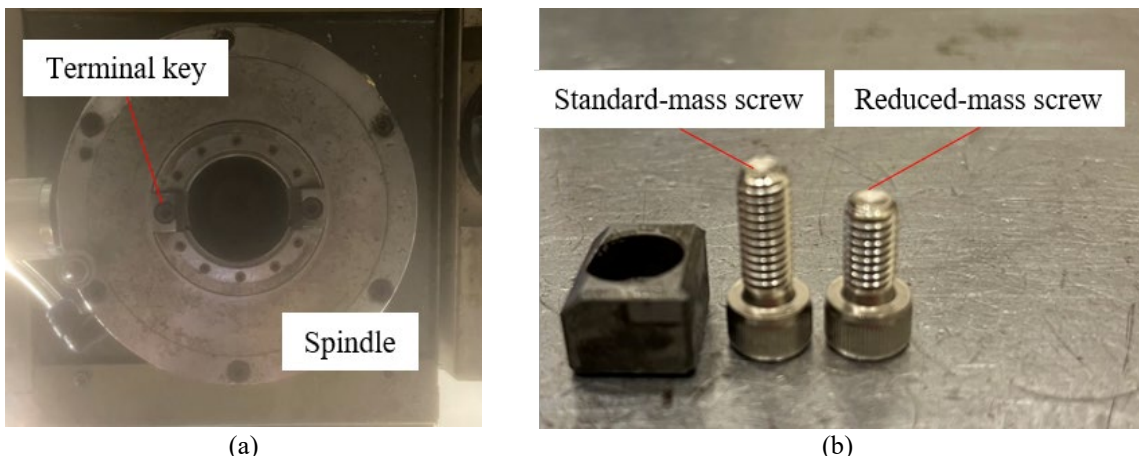


Fig. 2. Generation of spindle dynamic imbalance by altering the terminal key screw's mass: (a) screw installation position and (b) screw selection.

## THEORETICAL FRAMEWORK AND ANALYTICAL METHODS

### Feature Extraction

In this study, we performed feature extraction on each 1-s vibration signal. As shown in Table 3, the extracted features were primarily spindle rotation frequency features and bearing vibration features. For the spindle rotation frequency features, we used the spindle's rotational frequency as the fundamental frequency ( $f_d = 166.67$  Hz). Using fast Fourier transform (FFT), we extracted four features representing the spectral amplitudes of the fundamental frequency and its harmonic frequencies. These features effectively reflected the dynamic balance state of the spindle.

For the bearing vibration features, we conducted an envelope spectrum (enveloped-FFT spectrum) analysis, particularly because low contact stability between bearing components under spindle imbalance conditions can induce abnormal vibration, which

typically has intermittent or amplitude modulation characteristics (Rodet and Philippe, 1992). Envelope spectrum analyses demodulate and remove high-frequency carrier signals, highlighting low-frequency modulation signals and thereby making bearing-related characteristic frequencies more identifiable. Using this analysis, we extracted four key features from the envelope spectrum: the ball pass frequency outer (BPFO) amplitude, ball pass frequency inner (BPFI) amplitude, ball spin frequency (BSF) amplitude, and fundamental training frequency (FTF) amplitude.

In summary, we established a feature set containing eight frequency-domain features. These features were the key frequency components of both spindle rotation and bearing operation, thereby effectively characterizing the dynamic operational state of the spindle.

Table 3. Feature extraction methods and mathematical

expressions for spindle vibration analysis.

Feature	Expression	Description
$P_{nX}$	$s(n \times f_d)$ , $n = 1, 2, 3, 4$	Amplitudes corresponding to the harmonic frequencies of $n \times f_d$ in an FFT spectrum
$P_{BSF}$	Amplitude corresponding to a BSF of 1,876 Hz in an enveloped-FFT spectrum	
$P_{FTF}$	Amplitude corresponding to an FTF of 76 Hz in an enveloped-FFT spectrum	
$P_{BPF1}$	Amplitude corresponding to a BPF1 of 2,532 Hz in an enveloped-FFT spectrum	
$P_{BPF0}$	Amplitude corresponding to a BPF0 of 2,135 Hz in an enveloped-FFT spectrum	

\*Note:  $x_i = (x_1, x_2, \dots, x_N)$  is the sequence of the time-domain signal;  $s(k)$  is the amplitude corresponding to a frequency of  $k$  Hz in the FFT spectra of  $x_i$ .

### Feature Data Set Refinement Based on PCA

After features are extracted, refining the feature data set is essential for establishing a robust and efficient diagnostic model. Major collinearity may exist between the extracted features, and this interdependence among features not only increases computational complexity but also may lead to model redundancy, leading to poor diagnostic performance (Shekar et al., 2017). To address this problem, we conducted PCA (Wold et al., 1987) to achieve feature dimensionality reduction. This approach can effectively eliminate the collinearity between features while preserving the main information in the data, thereby ensuring linear independence between the features used to establish the diagnostic model.

Data preprocessing is essential before PCA is performed for dimensionality reduction. Different features may be recorded using differing units of measurement, and these scale differences may cause certain features to have a disproportionate influence during analysis (Geladi and Kowalski, 1986). To eliminate this possibility, we adopted  $z$ -score standardization, which involves subtracting the mean from each feature's original data and dividing by the standard deviation (Patro and Sahu, 2015). This standardization approach not only makes different features comparable but also enhances the accuracy and reliability of subsequent PCA. In accordance with the PCA principles, the  $z$ -score standardized feature data set  $\mathbf{X} \in \mathbb{R}^{m \times n}$  (where  $m$  represents the number of samples and  $n$  represents the number of features) can be expressed as

$$\mathbf{X} = \mathbf{tP}^T \quad (1)$$

In this equation,  $\mathbf{P}$  consists of a series of principal component loading vectors (PCLVs) and can be expressed as  $\mathbf{P} = [\mathbf{p}_1, \dots, \mathbf{p}_i, \dots, \mathbf{p}_n]$ , where  $\mathbf{p}_i$  represents the  $i$ th PCLV, which is the  $i$ th eigenvector of the autocorrelation matrix of  $\mathbf{X}$ , with  $\lambda_i$  being its corresponding eigenvalue. The magnitude of eigenvalues directly reflects the importance of

corresponding PCLVs in explaining the original data variance, with small eigenvalues indicating that variation in a specific direction primarily originates from noise and can therefore be ignored during dimensionality reduction. Meanwhile,  $\mathbf{t}$  consists of all principal component score vectors corresponding to the principal components and can be expressed as  $\mathbf{t} = [\mathbf{t}_1, \dots, \mathbf{t}_i, \dots, \mathbf{t}_n]$ . To quantify the contribution of each PCLV to the original data variance, we calculated the contribution rate  $f_j$  of each PCLV, which is the ratio of the eigenvalue of that principal component to the sum of all eigenvalues:

$$f_j = \frac{\lambda_j}{\sum_{i=1}^n \lambda_i}, j = 1, 2, \dots, n \quad (2)$$

We selected the most appropriate degree of dimensionality reduction given the cumulative contribution rate. The typical approach is to sort the contribution rates  $f_j$  from highest to lowest and to select the first  $r$  PCLVs whose cumulative contribution rate is above a predetermined threshold. This approach enables the original  $n$ -dimensional feature space to be reduced to  $r$  dimensions:

$$\mathbf{t}_r = \mathbf{Xp}_r, \quad (3)$$

where  $\mathbf{P}_r = [\mathbf{p}_1, \dots, \mathbf{p}_r]$  consists of the selected  $r$  PCLVs and  $\mathbf{t}_r$  is the new dimensionality-reduced feature data set.

### Development of a Detection Model Based on SOM

In this study, an SOM (Huang et al., 2007) was used as an unsupervised learning technique to detect spindle state anomalies. The SOM was selected because of its unique competitive learning mechanism, which can effectively project high-dimensional training samples onto a two-dimensional neuron grid while preserving topological relationships. This dimensionality-reduction mapping approach not only retains the key clustering characteristics of the training data but also yields intuitive and easily interpretable visualizations, thereby facilitating understanding and analysis of complex high-dimensional data relationships. Figure 3 illustrates the key steps in the SOM training process. During the learning process of an SOM, a key feature is its preservation of input space topological properties through neighborhood functions. This mechanism ensures that similar input patterns are mapped to adjacent neurons during training, thereby enabling the formation of meaningful local structures in the two-dimensional grid space. This topology-preserving characteristic makes SOMs particularly suitable for anomaly detection tasks, particularly because they can effectively capture nonlinear relationships and potential anomalous patterns in data.

In a trained SOM network, the network structure clearly depicts the relationships between neighboring

neurons. Because adjacent neurons have similar feature representations in the original input space, SOMs effectively reflect the inherent relationships and patterns in the input data. Each SOM neuron represents a weight vector, which after training essentially becomes a representative center point of input data clusters, providing key reference benchmarks for subsequent anomaly detection.

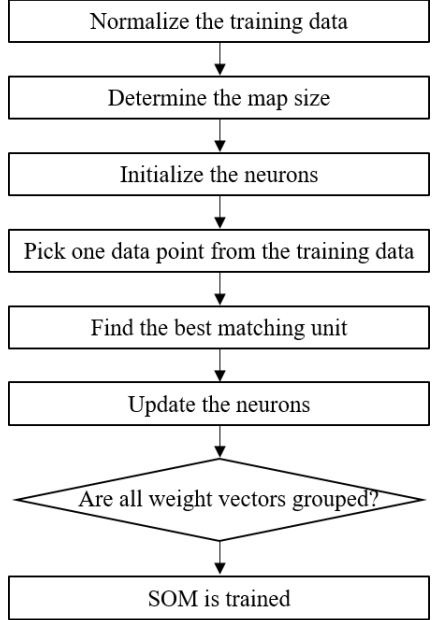


Fig. 3. Training process diagram for SOM.

## RESULTS AND DISCUSSION

To evaluate the effectiveness of the proposed method, we conducted a data analysis and validation experiment. We divided the collected data, which consisted of 51,750 normal spindle operation samples and 1,800 unbalanced spindle operation samples, into four feature subsets (A, B, C, and D) on the basis of their temporal characteristics (Table 4). Feature subsets A and B consisted of normal spindle operation data collected from April 8 to April 24 (randomly distributed at a ratio of 7:3), feature subset C consisted of normal spindle operation data collected from April 25 to May 9, and feature subset D consisted of unbalanced spindle operation data collected on April 16.

Figure 4 illustrates the overall training and testing process. In the model training phase, we used feature subset A to train the PCA model. Comprehensive analysis of the PCLV cumulative contribution rates revealed that the first five principal components achieved a cumulative contribution rate of 82% (Figure 5), which is widely accepted as a suitable threshold in engineering applications (Jolliffe, 1982). The sixth principal component would only contribute an additional 5% to the explained variance, while the remaining components collectively account

for less than 15% of the total variance. Given that this marginal increase in information retention does not justify the corresponding increase in computational complexity, these remaining components were reasonably regarded as influences on secondary variations. Therefore, we chose to retain the first five principal components for subsequent feature dimensionality reduction.

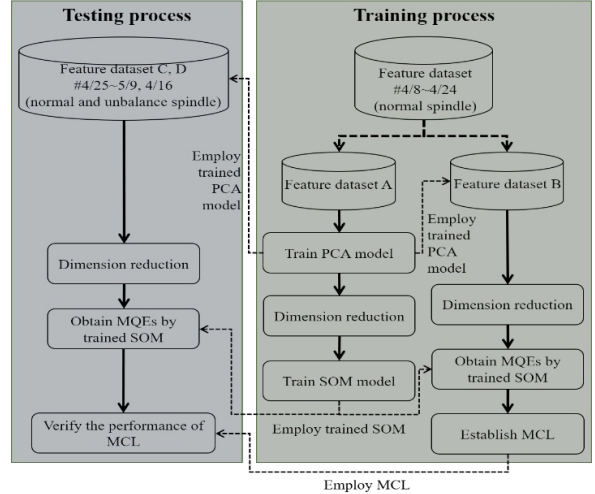


Fig. 4. Training and testing with feature subsets A, B, C, and D.

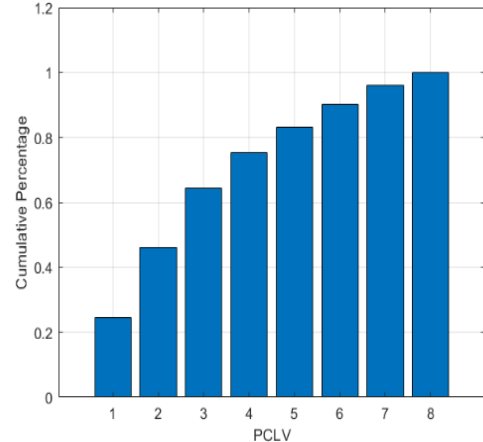


Fig. 5. PCLV selection.

After determining the optimal number of principal components, we selected feature subset A for PCA model dimensionality reduction, and we subsequently used this subset to train the SOM model. This SOM network structure design followed the empirical formula  $M \approx 5\sqrt{L}$  (Tian et al., 2014), where  $M$  represents the number of neurons and  $L$  represents the training data volume. For this study, we adopted a  $40 \times 40$  map size configuration with a total of 1,600 neurons and 400 training iterations. To establish reliable anomaly detection criteria, we proposed a monitoring control limit (MCL) method based on a minimum quantification error (MQE) (Huang et al.,

2007). We used the following equation to determine the MQE required for establishing the MCL:

$$MQE = \|\mathbf{d} - \mathbf{w}\|, \quad (4)$$

where  $\mathbf{d}$  represents the data obtained from feature subset B after PCA model dimensionality reduction and  $\mathbf{w}$  is the weight vector of the best matching unit in the SOM for feature subset B. Using the MQEs of feature subset B, we precisely quantified the difference between the input data and the training model. This quantification approach provided a reliable indicator of spindle state anomaly detection, enabling the system to identify potential spindle imbalance states in a timely manner. Overall, the MCL revealed two judgment thresholds, with differing levels of strictness, through the MQE distribution characteristics of feature subset B. These two thresholds were  $MCL_3$  and  $MCL_6$ , corresponding to the mean MQE plus three and six standard deviations, respectively:

$$MCL_3 = \mu + 3\sigma, \quad (5a)$$

$$MCL_6 = \mu + 6\sigma, \quad (5b)$$

where  $\sigma$  and  $\mu$  represent the standard deviation and mean, respectively, of the MQEs of feature subset B. Because the data in feature subset B all pertained to normal spindle operation, the MCL established with these data served as a threshold for distinguishing between healthy and unbalanced spindle states. Comparison of new samples with the established MCL led to these samples being classified as normal or unbalanced spindle states. According to our experimental results (Table 5), when  $MCL_6$  was used as the judgment threshold, the correct identification rate for feature subset C (normal spindle state) was 99.7%, and the correct identification rate for feature subset D (unbalanced spindle state) was 100%. These values represent a major improvement over the accuracy of 96.53% achieved when  $MCL_3$  was used, indicating that a more permissive threshold setting may be more suitable for practical applications.

To further confirm the effectiveness of the proposed method, we compared it with other traditional supervised learning techniques. Specifically, we selected a support vector machine (SVM) (Liua et al., 2019; Shuo et al., 2022) as our benchmark method, with a radial basis function as the kernel function to construct a classifier. Subsequently, we randomly divided feature subset D into D1 and D2 at a ratio of 1:1, with feature subsets A and D1 used for SVM model training and feature subsets C and D2 used for performance validation. The results indicated that although the SVM approach achieved high accuracy of 99.8% and 100% in identifying normal and unbalanced spindles, respectively, this supervised learning technique required training data from both normal and unbalanced states, which is often difficult

to achieve in practical applications. Notably, the computation time for establishing a diagnostic model was evaluated using an AMD Ryzen 9-5900HS (3.30 GHz, 32GB RAM) system. The model training time for SIDM and SVM methods were 13.4s and 4.5s, respectively, indicating that the SVM method reduces training time by 66%. By contrast, although the proposed method exhibited slightly lower accuracy in normal spindle judgment compared with the SVM approach (96.53% with  $MCL_3$  and 99.7% with  $MCL_6$ ), it enabled establishment of the diagnostic model and MCL judgment threshold on the basis of only vibration signals from normal spindle operation; data from unbalanced spindles were not required. This ability makes the proposed method more practical and universally applicable in industrial applications, particularly in scenarios in which fault data are difficult to obtain or undesirable to generate.

Table 4. Details of the four feature subsets.

Subset	Number of data points	Experiment date	Spindle status
A	13,860	April 8 to April 24	Normal
B	5,940	April 8 to April 24	Normal
C	31,950	April 25 to May 9	Normal
D	1,800	April 16	Unbalanced

Table 5. Detection results of the proposed method.

Subset	MCL <sub>3</sub>		MCL <sub>6</sub>	
	C	D	C	D
Actual spindle state	Normal	Unbalanced	Normal	Unbalanced
Classified as normal	30,841	0	31,855	0
Classified as unbalanced	1,109	1,800	95	1,800
Accuracy	96.53%	100%	99.7%	100%

## CONCLUSIONS

In this study, we developed and validated an SIDM to address the challenge of health monitoring for CNC machine tool spindles. Our main contributions and findings are summarized as follows:

- (1). The proposed feature extraction technique combines spindle rotation and bearing characteristic frequencies to effectively capture the dynamic characteristics of spindle operation. In addition, the integration of PCA for feature refinement successfully reduces data dimensionality while retaining 82% of the original information in the first five principal components.

- (2). The adoption of an SOM combined with an innovative MCL approach was found to result in high performance in distinguishing normal from unbalanced spindle states. In the case of MCL<sub>6</sub>, the proposed method achieves accuracy of 99.7% in normal state identification and 100% in imbalance detection, confirming the method's reliability in practical applications.
- (3). The proposed method performs similarly to traditional supervised learning techniques, such as SVMs, but it eliminates the need for fault data during model training. This ability makes the proposed method particularly valuable in industrial environments in which fault data are difficult to obtain or generate.

Overall, the proposed SIDM represents a major advancement in automated spindle health monitoring, providing a practical solution for improving maintenance efficiency and reducing machine downtime in modern manufacturing facilities.

## ACKNOWLEDGMENT

This study was supported by the Precision Machinery Research Development Center and the National Science and Technology Council of Taiwan (contract no. NSTC-113-2221-E-150-033).

## REFERENCES

Cao, H., Zhang, X., and Chen, X., "The Concept and Progress of Intelligent Spindles: A Review," *Int. J. Mach. Tools Manuf.*, Vol. 112, pp. 21-52(2017).

Dai, Y., Tao, X., Li, Z., Zhan, S., Li, Y., and Gao, Y., "A Review of Key Technologies for High-Speed Motorized Spindles of CNC Machine Tools," *Machines*, Vol. 10, No. 2, p. 145 (2022).

Gangsar, P., and Tiwari, R., "Signal Based Condition Monitoring Techniques for Fault Detection and Diagnosis of Induction Motors: A State-of-the-Art Review," *Mech. Syst. Signal Process.*, Vol. 144, p. 106908(2020).

Hsieh, N.K., Lin, W.Y., and Young, H.T., "High-Speed Spindle Fault Diagnosis with the Empirical Mode Decomposition and Multiscale Entropy Method," *Entropy*, Vol. 17, No. 4, pp. 2170-2183(2015).

Denkena, B., Dittrich, M.A., Noske, H., Stoppel, D., and Lange, D., "Data-Based Ensemble Approach for Semi-Supervised Anomaly Detection in Machine Tool Condition Monitoring," *CIRP J. Manuf. Sci. Technol.*, Vol. 35, pp. 795-802(2021).

Fernandes, M., Corchado, J.M., and Marreiros, G., "Machine Learning Techniques Applied to Mechanical Fault Diagnosis and Fault Prognosis in the Context of Real Industrial Manufacturing Use-Cases: A Systematic Literature Review," *Appl. Intell.*, Vol. 52, No. 12, pp. 14246-14280(2022).

Geladi, P., and Kowalski, B.R., "Partial Least-Squares Regression: A Tutorial," *Anal. Chim. Acta*, Vol. 185, pp. 1-17(1986).

Hassan, I.U., Panduru, K., and Walsh, J., "Review of Data Processing Methods Used in Predictive Maintenance for Next Generation Heavy Machinery," *Data*, Vol. 9, No. 5, pp. 69(2024).

Huang, P., Lee, W.B. and Chan, C.Y., "Investigation of the Effects of Spindle Unbalance Induced Error Motion on Machining Accuracy in Ultra-Precision Diamond Turning," *Int. J. Mach. Tools Manuf.*, Vol. 94, pp. 48-56(2015).

Huang, R., Xi, L., Li, X., Liu, C.R., Qiu, H. and Lee, J., "Residual Life Predictions for Ball Bearings Based on Self-Organizing Map and Back Propagation Neural Network Methods," *Mech. Syst. Signal Process.*, Vol. 21, No. 1, pp. 193-207(2007).

Jolliffe, I.T., "A note on the use of principal components in regression," *Journal of the Royal Statistical Society. Series C (Applied Statistics)*, Vol. 31, No. 3, pp. 300-303(1982).

Kuntoğlu, M., M., Salur, E., Gupta, M.K., Sarıkaya, M., and Pimenov, D.Y., "A State-of-the-Art Review on Sensors and Signal Processing Systems in Mechanical Machining Processes," *Int. J. Adv. Manuf. Technol.*, Vol. 116, No. 9, pp. 2711-2735(2021).

Liua, J.Y., Yub, X.G., and Hana, Q.K., "Research on Fault Diagnosis of Aeronautic Gear Based on Permutation Entropy and SVM Method," *J. Chin. Soc. Mech. Eng.*, Vol. 40, No. 4, pp. 413-422(2019).

Ma, W., Liu, X., Yue, C., Wang, L., and Liang, S.Y., "Multi-Scale One-Dimensional Convolution Tool Wear Monitoring Based on Multi-Model Fusion Learning Skills," *J. Manuf. Syst.*, Vol. 70, pp. 69-98(2023).

Olalere, I.O., and Olanrewaju, O.A., "Tool and Workpiece Condition Classification Using Empirical Mode Decomposition (EMD) with Hilbert–Huang Transform (HHT) of Vibration Signals and Machine Learning Models," *Appl. Sci.*, Vol. 13, No. 4, pp. 2248(2023).

Rodet, X., and Philippe, D., "Spectral Envelopes and Inverse FFT Synthesis," *93rd Audio Eng. Soc. Convention* (1992).

Patro, S.G.K., and Sahu, K.K., "Normalization: A Preprocessing Stage," *arXiv preprint arXiv:1503.06462* (2015).

Peng, F., Zheng, L., Peng, Y., Fang, C., and Meng, X., "Digital Twin for Rolling Bearings: A Review of Current Simulation and PHM

Techniques," *Measurement*, Vol. 201, pp. 111728(2022).

Shekar, A.K., Bocklisch, T., Sánchez, P.I., Straehle, C.N., and Müller, E., "Including Multi-Feature Interactions and Redundancy for Feature Ranking in Mixed Datasets," In Joint European Conference on Machine Learning and Knowledge Discovery in Databases, LNAI (10534), pp. 239-255(2017).

Shuo, W.A.N.G., Zhenliang, Y.U., Xu, L.I.U., and Zhipeng, L.Y.U., "Fault Monitoring and Diagnosis of Motorized Spindle in Five-Axis Machining Center Based on CNN-SVM-PSO," *Mech. Eng. Sci.*, Vol. 4 No. 2, pp. 21-29(2022).

Tama, B.A., Vania, M., Lee, S., and Lim, S., "Recent Advances in the Application of Deep Learning for Fault Diagnosis of Rotating Machinery Using Vibration Signals," *Artif. Intell. Rev.*, Vol. 56, No. 5, 4667-4709(2023).

Thoppil, N.M., Vasu, V., and Rao, C.S.P., "Bayesian Optimization LSTM/bi-LSTM Network with Self-Optimized Structure and Hyperparameters for Remaining Useful Life Estimation of Lathe Spindle Unit," *J. Comput. Inf. Sci. Eng.*, Vol. 22 No. 2, p. 021012(2022).

Tian, J., Azarian, M.H., and Pecht, M., "Anomaly Detection Using Self-Organizing Maps-Based K Nearest Neighbor Algorithm," *PHM Soc. Eur. Conf.*, Vol. 2. No. 1(2014).

Wold, S., Esbensen, K., and Geladi, P., "Principal Component Analysis," *Chemom. Intell. Lab. Syst.*, Vol. 2, Nos. 1-3, pp. 37-52(1987).

Wójcicki, J., Leonesio, M., and Bianchi, G., "Potential for Smart Spindles Adoption as Edge Computing Nodes in Industry 4.0," *Procedia CIRP*, Vol. 99, pp. 86-91(2021).

Wong, S.Y., Chuah, J.H., and Yap, H.J., "Technical Data-Driven Tool Condition Monitoring Challenges for CNC Milling: A Review," *Int. J. Adv. Manuf. Technol.*, Vol. 107, pp. 4837-4857(2020).

Zheng, Q., Chen, G., and Jiao, A., "Chatter Detection in Milling Process Based on the Combination of Wavelet Packet Transform and PSO-SVM," *Int. J. Adv. Manuf. Technol.*, Vol. 120, No. 1, pp. 1237-1251(2022).